

Sketch-and-Project Meets Newton Method: Global $\mathcal{O}(k^{-2})$ Convergence with Low-Rank Updates

Slavomír Hanzely*

Abstract

In this paper, we propose the first sketch-and-project Newton method with fast $\mathcal{O}(k^{-2})$ global convergence rate for self-concordant functions. Our method, SGN, can be viewed in three ways: i) as a sketch-and-project algorithm projecting updates of Newton method, ii) as a cubically regularized Newton method in sketched subspaces, and iii) as a damped Newton method in sketched subspaces.

SGN inherits best of all three worlds: cheap iteration costs of sketch-and-project methods, state-of-the-art $\mathcal{O}(k^{-2})$ global convergence rate of full-rank Newton-like methods and the algorithm simplicity of damped Newton methods. Finally, we demonstrate its comparable empirical performance to baseline algorithms.

1 Introduction

Second-order methods have always been a fundamental component of both scientific and industrial computing. Their origins can be traced back to the works Newton [1687], Raphson [1697], and Simpson [1740], and they have undergone extensive development throughout history [Kantorovich, 1948, Moré, 1978, Griewank, 1981]. For the more historical development of classical methods, we refer the reader to [Ypma, 1995]. The amount of practical applications is enormous, with over a thousand papers included in the survey Conn et al. [2000] on trust-region and quasi-Newton methods alone.

Second-order methods are highly desirable due to their invariance to rescaling and coordinate transformations, which significantly reduces the complexity of hyperparameter tuning. Moreover, this invariance allows convergence independent of the conditioning of the underlying problem. In contrast, the convergence rate of first-order methods is fundamentally dependent on the function conditioning. Moreover, first-order methods can be sensitive to variable parametrization and function scale, hence parameter tuning (e.g., step size) is often crucial for efficient execution.

On the other hand, even the simplest and most classical second-order method, Newton’s method [Kantorovich, 1948], achieves an extremely fast, quadratic convergence rate (precision doubles in each iteration) [Nesterov and Nemirovski, 1994] when initialized sufficiently close to the solution. However, the convergence of the Newton method is limited only to the neighborhood of the solution. Several works, including Jarre and Toint [2016], Mascarenhas [2007], Bolte and Pauwels [2022] demonstrate that when initialized far from optimum, the line search and trust-region Newton-like method can diverge on both convex and nonconvex problems.

1.1 Demands of modern machine learning

Despite the long history of the field, research on second-order methods has been thriving to this day. Newton-like methods with a fast $\mathcal{O}(k^{-2})$ global rate were introduced relatively recently under the name Globally Regularized Newton methods [Nesterov and Polyak, 2006, Doikov and Nesterov, 2022, Mishchenko, 2021, Hanzely et al., 2022]. The main limitation of these methods is their poor

*King Abdullah University of Science and Technology, Saudi Arabia

Table 1: Global convergence rates of low-rank Newton methods for convex and Lipschitz smooth functions. For simplicity, we disregard differences between various notions of smoothness. We use **fastest** full-dimensional algorithms as the baseline. For extended version, see Section 4.

Update oracle Update direction	Full-dimensional (direction is deterministic)	Low-rank (direction in expectation)
Non-Newton direction	$\mathcal{O}(k^{-2})$ Cubic Newton [Nesterov and Polyak, 2006] Glob. Regularized Newton [Mishchenko, 2021] [Doikov and Nesterov, 2021]	$\mathcal{O}(k^{-1})$ Stoch. Subspace Cubic Newton [Hanzely et al., 2020]
Newton direction	$\mathcal{O}(k^{-2})$ Affine-Invariant Cubic Newton [Hanzely et al., 2022]	$\mathcal{O}(k^{-2})$ Sketchy Global Newton (this work) $\mathcal{O}(k^{-1})$ Randomized Subspace Newton [Gower et al., 2019]

Algorithm 1 SGN: Sketchy Global Newton (**new**)

- 1: **Requires:** Initial point $x_0 \in \mathbb{R}^d$, distribution of sketch matrices \mathcal{D} , constant $L_{\text{est}} \geq \sup_{\mathbf{S} \sim \mathcal{D}} L_{\mathbf{S}}$
 - 2: \triangleright Choice $L_{\text{est}} \geq 1.2 \sup_{\mathbf{S}} L_{\mathbf{S}} \hat{L}_{\mathbf{S}}^2 > 0$ yields global linear rate for relative convex f
 - 3: **for** $k = 0, 1, 2 \dots$ **do**
 - 4: Sample $\mathbf{S}_k \sim \mathcal{D}$
 - 5:
$$\alpha_{k,\mathbf{S}} = \frac{-1 + \sqrt{1 + 2L_{\text{est}} \|\nabla_{\mathbf{S}_k} f(x_k)\|_{x_k, \mathbf{S}_k}^*}}{L_{\text{est}} \|\nabla_{\mathbf{S}_k} f(x_k)\|_{x_k, \mathbf{S}_k}^*}$$
 - 6: $x_{k+1} = x_k - \alpha_{k,\mathbf{S}} \mathbf{S}_k [\nabla_{\mathbf{S}_k}^2 f(x_k)]^\dagger \nabla_{\mathbf{S}_k} f(x_k)$ \triangleright Equivalent updates are (5) and (7).
 - 7: **end for**
-

scalability for modern large-scale machine learning. Large datasets with numerous features necessitate well-scalable algorithms. While tricks or inexact approximations can be used to avoid computing the inverse Hessian, simply storing the Hessian becomes impractical when the dimensionality d is large. This motivated recent developments; works Qu et al. [2016], Luo et al. [2016], Gower et al. [2019], Doikov and Richtárik [2018], and Hanzely et al. [2020] propose Newton-like method operating in random low-dimensional subspaces. This approach is also known as sketch-and-project Gower and Richtárik [2015]. It reduces iteration cost drastically, but for the cost of slower, $\mathcal{O}(k^{-1})$ convergence rate [Gower et al., 2020], [Hanzely et al., 2020].

1.2 Contributions

In this work, we argue that those sketch-and-project adaptations of second-order can be improved. We propose a **first sketch-and-project** method (Sketchy Global Newton, **SGN**, Algorithm 1) with fast $\mathcal{O}(k^{-2})$ global convex convergence rate – matching global fast rate of full-dimensional Globally regularized Newton methods (as summarized in Table 1). In particular, sketching on $\mathcal{O}(1)$ -dimensional subspaces leads to $\mathcal{O}(k^{-2})$ global convex convergence with an iteration cost $\mathcal{O}(1)$. As a cherry on top, we additionally show **i)** local linear rate independent on the condition number, **ii)** global linear convergence under relative convexity assumption. We summarize the contributions below and in Tables 2, 3:

- **One connects all:** We present **SGN** through three orthogonal viewpoints: sketch-and-project method, subspace Newton method with stepsize, and Regularized Newton method. Compared to established algorithms, **SGN** is AICN in subspaces, SSCN in local norms, and RSN with a stepsize schedule.

- **Fast global convergence:** **SGN** is first low-rank method that solves **convex** functions with $\mathcal{O}(k^{-2})$ global rate (Theorem 2). This matches state-of-the-art rates of full-rank Newton-like methods. Other sketch-and-project methods, in particular, SSCN and RSN have slower $\mathcal{O}(k^{-1})$ rate.

- **Cheap iterations:** **SGN** uses τ -dimensional updates. Naively implemented, its per-iteration cost is proportional to τ^3 while full-rank Newton methods have cost proportional to d^3 and $d \gg \tau$.

• **Linear local rate:** **SGN** has local linear rate $\mathcal{O}\left(\frac{d}{\tau} \log \frac{1}{\varepsilon}\right)$ (Theorem 3) dependent only on the ranks of the sketching matrices. This improves over the condition-dependent linear rate of RSN or any rate of first-order methods.

• **Global linear rate:** Under $\hat{\mu}$ -relative convexity, **SGN** achieves global linear rate $\mathcal{O}\left(\frac{L_{\text{est}}}{\rho\hat{\mu}} \log \frac{1}{\varepsilon}\right)^1$ to a neighborhood of the solution (Theorem 4).

• **Geometry and interpretability:** Update of **SGN** uses well-understood projections² of Newton method with stepsize schedule AICN. Moreover, those stochastic projections are affine-invariant and in expectation preserve direction (1). On the other hand, implicit steps of regularized Newton methods including SSCN lack geometric interpretability.

• **Algorithm simplicity:** **SGN** is affine-invariant and independent of the choice of the basis. This removes one parameter from potential parameter tuning. Update rule (6) is simple and explicit. Conversely, most of the fast globally-convergent Newton-like algorithms require an extra subproblem solver in each iteration.

• **Analysis:** The analysis of **SGN** is simple, all steps have clear geometric interpretation. On the other hand, the analysis of SSCN [Hanzely et al., 2020] is complicated as it measures distances in both l_2 norms and local norms. This not only makes it harder to understand but also leads to worse constants, which ultimately cause a slower convergence rate.

¹ ρ is condition number of projection matrix, (33) and L_{est} is constant affecting stepsize, (9).

²Gower et al. [2020] describes six equivalent viewpoints.

Table 2: Three approaches for second-order global minimization. We denote $x_k \in \mathbb{R}^d$ model iterates, $\mathbf{S}_k \sim \mathcal{D}$ distribution of sketch matrices with rank $\tau \ll d$, $\alpha_k, \alpha_{k, \mathbf{S}_k}$ stepsizes, $L_2, L_{\mathbf{S}}$ smoothness constants, c_{stab} Hessian stability constant. For simplicity, we disregard differences in assumptions. We report algorithm complexities when matrix inverses are naively implemented.

Orthogonal lines of work	Sketch-and-Project [Gower and Richtárik, 2015] (various update rules)	Damped Newton [Nesterov and Nemirovski, 1994] [Karimireddy et al., 2018]	Globally Regularized Newton ^(r) [Nesterov and Polyak, 2006] [Polyak, 2009] [Mishchenko, 2021] [Doikov and Nesterov, 2021]
Update $x_{k+1} - x_k =$	$\alpha_{k, \mathbf{S}_k} \mathbf{P}_{x_k}^{\mathbf{S}_k}(\text{update}(x_k))$, for $\mathbf{S}_k \sim \mathcal{D}$	$\alpha_k [\nabla^2 f(x_k)]^\dagger \nabla f(x_k)$	$\text{argmin}_{h \in \mathbb{R}^d} T(x_k, h)$, for $T(x, h) \stackrel{\text{def}}{=} \langle \nabla f(x), h \rangle +$ $+\frac{1}{2} \ h\ _x^2 + \frac{L_2}{6} \ h\ _x^3$
Characteristics	+ cheap, low-rank updates + global linear convergence (conditioning-dependent) - optimal rate: linear	+ affine-invariant geometry - iteration cost $\mathcal{O}(d^3)$ Fixed $\alpha_k = c_{\text{stab}}^{-1}$: + global linear convergence Schedule $\alpha_k \nearrow 1$: + local quadratic rate	+ global convex rate $\mathcal{O}(k^{-2})$ + local quadratic rate - implicit updates - iteration cost $\mathcal{O}(d^3 \log \frac{1}{\varepsilon})$ + local quadratic rate
Combinations + retained benefits	Sketch-and-Project	Damped Newton	Globally Regularized Newton
RSN [Gower et al., 2019] Algorithm 3	✓ + iteration cost $\mathcal{O}(\tau^3)$	✓ + global rate $\mathcal{O}\left(\frac{1}{\rho} \frac{L_2}{\hat{\mu}} \log \frac{1}{\varepsilon}\right)$	✗
SSCN [Hanzely et al., 2020] Algorithm 4	✓ + iteration cost $\mathcal{O}(\tau^3 \log \frac{1}{\varepsilon})$ + local rate $\mathcal{O}\left(\frac{d}{\tau} \log \frac{1}{\varepsilon}\right)$	✗	✓ + global convex rate $\mathcal{O}(k^{-2})$
AICN [Hanzely et al., 2022] Algorithm 5	✗	✓ + affine-invariant geometry - no global linear rate proof ^(lim)	✓ + global convex rate $\mathcal{O}(k^{-2})$ + local quadratic rate + iteration cost $\mathcal{O}(d^3)$ + simple, explicit updates
SGN (this work) Algorithm 1	✓ + iteration cost $\mathcal{O}(\tau^3 \log \frac{1}{\varepsilon})$ + local rate $\mathcal{O}\left(\frac{d}{\tau} \log \frac{1}{\varepsilon}\right)$ - quadratic rate unachievable	✓ + affine-invariant geometry + global rate $\mathcal{O}\left(\frac{1}{\rho} \frac{L_2}{\hat{\mu}} \log \frac{1}{\varepsilon}\right)$	✓ + global convex rate $\mathcal{O}(k^{-2})$ + simple, explicit updates
Three descriptions of SGN	Sketch-and-Project of Damped Newton method	Damped Newton in sketched subspaces	Affine-Invariant Cubic Newton in sketched subspaces
Update $x_{k+1} - x_k =$	$\alpha_{k, \mathbf{S}_k} \mathbf{P}_{x_k}^{\mathbf{S}_k} [\nabla^2 f(x_k)]^\dagger \nabla f(x_k)$	$\alpha_{k, \mathbf{S}_k} \mathbf{S}_k [\nabla_{\mathbf{S}_k} f(x_k)]^\dagger \nabla_{\mathbf{S}_k} f(x_k)$	$\mathbf{S}_k \text{argmin}_{h \in \mathbb{R}^d} T_{\mathbf{S}_k}(x_k, h)$, for $T_{\mathbf{S}}(x, h) \stackrel{\text{def}}{=} \langle \nabla f(x), \mathbf{S}h \rangle +$ $+\frac{1}{2} \ \mathbf{S}h\ _x^2 + \frac{L_{\mathbf{S}}}{6} \ \mathbf{S}h\ _x^3$

^(r) Works Polyak [2009], Mishchenko [2021], Doikov and Nesterov [2021] have explicit updates and iteration cost $\mathcal{O}(d^3)$, but for the costs of slower global rate, slower local rate, and slower local rate, respectively.

^(lim) [Hanzely et al., 2022] didn't show global linear rate of AICN. However, it follows from our Theorems 4, 3 for $\mathbf{S}_k = \mathbf{I}$.

Table 3: Globally convergent Newton-like methods. For simplicity, we disregard differences and assumptions - we assume strong convexity, L -smoothness, semi-strong self-concordance and bounded level sets. We highlight the best know rates in blue.

Algorithm	Stepsize range	Affine invariant algorithm?	Iteration cost ^(dim)	Linear ^(lin) convergence	Global convex convergence	Reference
Newton	1	✓	$\mathcal{O}(d^3)$	✗	✗	Kantorovich [1948]
Damped Newton B	(0, 1]	✓	$\mathcal{O}(d^3)$	✗	$\mathcal{O}(k^{-\frac{1}{2}})$	Nesterov and Nemirovski [1994]
AICN	(0, 1]	✓	$\mathcal{O}(d^3)$	✗	$\mathcal{O}(k^{-2})$	[Hanzely et al., 2022]
Cubic Newton	1	✗	$\mathcal{O}(d^3 \log \frac{1}{\varepsilon})^{(\text{imp})}$	✗	$\mathcal{O}(k^{-2})$	Nesterov and Polyak [2006]
Glob. Reg. Newton	1	✗	$\mathcal{O}(d^3)$	✗	$\mathcal{O}(k^{-\frac{1}{4}})$	Polyak [2009]
Glob. Reg. Newton	1	✗	$\mathcal{O}(d^3)$	✗	$\mathcal{O}(k^{-2})$	Mishchenko [2021] Doikov and Nesterov [2021]
Exact Newton Descent	$\frac{1}{L}^{(c)}$	✓	$\mathcal{O}(d^3)$	glob ^(c)	✗	Karimireddy et al. [2018]
RSN	$\frac{1}{L}$	✓	$\mathcal{O}(\tau^3)$	glob ^(c)	$\mathcal{O}(k^{-1})$	Gower et al. [2019]
SSCN	1	✗	$\mathcal{O}(\tau^3 \log \frac{1}{\varepsilon})^{(\text{imp})}$	loc	$\mathcal{O}(k^{-1})$	Hanzely et al. [2020]
SGN (our)	(0, 1]	✓	$\mathcal{O}(\tau^3)$	loc + glob ^(sep)	$\mathcal{O}(k^{-2})$	This work

^(dim) d is function dimension, τ is rank of sketch matrices $\mathbf{S} \in \mathbb{R}^{d \times \tau}$. We report rate of implementation using matrix inverses.

^(lin) "loc" and "glob" denotes whether algorithms have local and global linear rate (under possibly stronger assumptions).

^(imp) Cubic Newton and SSCN solve implicit problem each iteration. Naively implemented, it requires $\times \log \frac{1}{\varepsilon}$ matrix inverses to approximate sufficiently in order to converge to ε -neighborhood [Hanzely et al., 2022].

^(c) Authors assume c -stability, which is implied by Lipschit smoothness + strong convexity. [Gower et al., 2019]

^(sep) Separate results for local convergence (Theorem 3) and global convergence to corresponding neighborhood (Theorem 4).

1.3 Notation

Our paper requires a nontrivial amount of notation. To facilitate reference, we will highlight new definitions in gray and theorems in light blue. We consider the optimization objective

$$\min_{x \in \mathbb{R}^d} f(x), \quad (1)$$

where f is convex, twice differentiable, bounded from below, and potentially ill-conditioned. The number of features d is potentially large. Subspace methods use a sparse update

$$x_+ = x + \mathbf{S}h, \quad (2)$$

where $\mathbf{S} \in \mathbb{R}^{d \times \tau(\mathbf{S})}$, $\mathbf{S} \sim \mathcal{D}$ is a thin matrix and $h \in \mathbb{R}^{\tau(\mathbf{S})}$. We denote gradients and Hessians along the subspace spanned by columns of \mathbf{S} as $\nabla_{\mathbf{S}} f(x) \stackrel{\text{def}}{=} \mathbf{S}^\top \nabla f(x)$ and $\nabla_{\mathbf{S}}^2 f(x) \stackrel{\text{def}}{=} \mathbf{S}^\top \nabla^2 f(x) \mathbf{S}$.

Also, denote any minimizer of function f as $x_* \stackrel{\text{def}}{=} \operatorname{argmin}_{x \in \mathbb{R}^d} f(x)$ and its value $f_* \stackrel{\text{def}}{=} f(x_*)$.

We can define norms based on a symmetric positive definite matrix $\mathbf{H} \in \mathbb{R}^{d \times d}$:

$$\|x\|_{\mathbf{H}} \stackrel{\text{def}}{=} \langle \mathbf{H}x, x \rangle^{1/2}, \quad x \in \mathbb{R}^d, \quad \|g\|_{\mathbf{H}}^* \stackrel{\text{def}}{=} \langle g, \mathbf{H}^{-1}g \rangle^{1/2}, \quad g \in \mathbb{R}^d.$$

As a special case $\mathbf{H} = \mathbf{I}$, we get l_2 norm $\|x\|_{\mathbf{I}} = \langle x, x \rangle^{1/2}$. We will be using local Hessian norm $\mathbf{H} = \nabla^2 f(x)$, with shorthand notation

$$\|h\|_x \stackrel{\text{def}}{=} \langle \nabla^2 f(x)h, h \rangle^{1/2}, \quad h \in \mathbb{R}^d, \quad \|g\|_x^* \stackrel{\text{def}}{=} \langle g, \nabla^2 f(x)^{-1}g \rangle^{1/2}, \quad g \in \mathbb{R}^d. \quad (3)$$

As we will be restricting iteration steps to subspaces, we will work with $\|h\|_{x,\mathbf{S}} = \|h\|_{\nabla_{\mathbf{S}}^2 f(x)}$.

For a matrix $\mathbf{H} \in \mathbb{R}^{d \times d}$ and a fixed $x \in \mathbb{R}^d$, operator norm is defined by

$$\|\mathbf{H}\|_{op} \stackrel{\text{def}}{=} \sup_{v \in \mathbb{E}} \frac{\|\mathbf{H}v\|_x^*}{\|v\|_x}. \quad (4)$$

Note that the operator norm of Hessian in the corresponding point x is one, $\|\nabla^2 f(x)\|_{op} = 1$.

2 Algorithm

2.1 Three faces of the algorithm

Our algorithm combines the best of three worlds (Table 2) and we can write it in three different ways.

Theorem 1 (SGN). *If $\nabla f(x_k) \in \text{Range}(\nabla^2 f(x_k))$ then following update rules are equivalent:*

$$\text{Cubically Regularized Newton step: } x_{k+1} = x_k + \mathbf{S}_k \underset{h \in \mathbb{R}^d}{\text{argmin}} T_{\mathbf{S}_k}(x_k, h), \quad (5)$$

$$\text{Damped Newton step: } x_{k+1} = x_k - \alpha_{k,\mathbf{S}_k} \mathbf{S}_k [\nabla_{\mathbf{S}_k}^2 f(x_k)]^\dagger \nabla_{\mathbf{S}_k} f(x_k), \quad (6)$$

$$\text{Sketch-and-project step: } x_{k+1} = x_k - \alpha_{k,\mathbf{S}_k} \mathbf{P}_{x_k}^{\mathbf{S}_k} [\nabla^2 f(x_k)]^\dagger \nabla f(x_k), \quad (7)$$

where $\mathbf{P}_x^{\mathbf{S}}$ is a projection matrix on $\text{Range}(\mathbf{S})$ w.r.t. norm $\|\cdot\|_x$ (defined in eq. (13)),

$$\begin{aligned} T_{\mathbf{S}}(x, h) &\stackrel{\text{def}}{=} f(x) + \langle \nabla f(x), \mathbf{S}h \rangle + \frac{1}{2} \|\mathbf{S}h\|_x^2 + \frac{L_{est}}{6} \|\mathbf{S}h\|_x^3 \\ &= f(x) + \langle \nabla_{\mathbf{S}} f(x), h \rangle + \frac{1}{2} \|h\|_{x,\mathbf{S}}^2 + \frac{L_{est}}{6} \|h\|_{x,\mathbf{S}}^3, \end{aligned} \quad (8)$$

$$\alpha_{k,\mathbf{S}} \stackrel{\text{def}}{=} \frac{-1 + \sqrt{1 + 2L_{est} \|\nabla_{\mathbf{S}} f(x_k)\|_{x_k,\mathbf{S}}^*}}{L_{est} \|\nabla_{\mathbf{S}} f(x_k)\|_{x_k,\mathbf{S}}^*}. \quad (9)$$

We call this algorithm *Sketchy Global Newton, SGN*, as in Algorithm 1.

Notice $\alpha_{k,\mathbf{S}_k} \in (0, 1]$ and $\alpha_{k,\mathbf{S}_k} \xrightarrow{L_{est} \|\nabla_{\mathbf{S}_k} f(x_k)\|_{x_k,\mathbf{S}_k}^* \rightarrow 0} 1$ and $\alpha_{k,\mathbf{S}_k} \xrightarrow{L_{est} \|\nabla_{\mathbf{S}_k} f(x_k)\|_{x_k,\mathbf{S}_k}^* \rightarrow \infty} 0$.

For **SGN**, we can transition between gradients and model differences $h_k \stackrel{\text{def}}{=} x_{k+1} - x_k$ by identities

$$h_k \stackrel{(6)}{=} -\alpha_{k,\mathbf{S}_k} \mathbf{S}_k [\nabla_{\mathbf{S}_k}^2 f(x_k)]^\dagger \nabla_{\mathbf{S}_k} f(x_k), \quad \|h_k\|_{x_k} = \alpha_{k,\mathbf{S}_k} \|\nabla_{\mathbf{S}_k} f(x_k)\|_{x_k,\mathbf{S}_k}^*. \quad (10)$$

2.2 Invariance to affine transformations

We will use assumptions that are invariant to the problem scale and choice of basis. An affine-invariant version of smoothness is called self-concordance, we will formulate it in sketched spaces.

Definition 1. *Convex function $f \in C^3$ is $L_{\mathbf{S}}$ -self-concordant in range of \mathbf{S} if*

$$L_{\mathbf{S}} \stackrel{\text{def}}{=} \max_{x \in \mathbb{R}^d} \max_{\substack{h \in \mathbb{R}^{\tau(\mathbf{S})} \\ h \neq 0}} \frac{|\nabla^3 f(x)[\mathbf{S}h]^3|}{\|\mathbf{S}h\|_x^3}, \quad (11)$$

where $\nabla^3 f(x)[h]^3 \stackrel{\text{def}}{=} \nabla^3 f(x)[h, h, h]$ is 3-rd order directional derivative of f at x along $h \in \mathbb{R}^d$.

In case $\mathbf{S} = \mathbf{I}$, Definition 1 matches definition of self-concordance and $L_{\mathbf{S}} \leq L_{sc}$. We will also use a slightly stronger version, semi-strong self-concordance, introduced in Hanzely et al. [2022].

Definition 2. Convex function $f \in C^2$ is called semi-strongly self-concordant if

$$\|\nabla^2 f(y) - \nabla^2 f(x)\|_{op} \leq L_{semi} \|y - x\|_x, \quad \forall y, x \in \mathbb{R}^d. \quad (12)$$

Proposition 1 (Lemma 2.2 Hanzely et al. [2020]). Constant L_S is determined from $\text{Range}(\mathbf{S})$, and $\text{Range}(\mathbf{S}) = \text{Range}(\mathbf{S}')$ implies $L_S = L_{S'}$.

2.3 Geometry of sketches

We will use a projection matrix on subspaces \mathbf{S} w.r.t. to local norms $\|\cdot\|_x$. Denote

$$\mathbf{P}_x^{\mathbf{S}} \stackrel{\text{def}}{=} \mathbf{S} (\mathbf{S}^\top \nabla^2 f(x) \mathbf{S})^\dagger \mathbf{S}^\top \nabla^2 f(x). \quad (13)$$

Lemma 1 (Gower et al. [2020]). Matrix $\mathbf{P}_x^{\mathbf{S}}$ is a projection matrix on $\text{Range}(\mathbf{S})$ w.r.t. norm $\|\cdot\|_x$.

We aim **SGN** to preserve Newton's direction in expectation. In view of (7), we can see that this holds as long $\mathbf{S} \sim \mathcal{D}$ is such that its projection is unbiased in expectation.

Assumption 1. For distribution \mathcal{D} there exists $\tau > 0$, so that

$$\mathbb{E}_{\mathbf{S} \sim \mathcal{D}} [\mathbf{P}_x^{\mathbf{S}}] = \frac{\tau}{d} \mathbf{I}. \quad (14)$$

Lemma 2. Assumption 1 implies $\mathbb{E}_{\mathbf{S} \sim \mathcal{D}} [\tau(\mathbf{S})] = \tau$.

Note that Assumption 1 is formulated in the local norm, so it might seem restrictive. Next lemma demonstrates that such sketching matrices can be obtained from sketches with l_2 -unbiased projection (which were used in [Hanzely et al., 2020]).

Lemma 3 (Construction of sketch matrix \mathbf{S}). If we have a sketch matrix distribution $\tilde{\mathcal{D}}$ so that a projection on $\text{Range}(\mathbf{M})$, $\mathbf{M} \sim \tilde{\mathcal{D}}$ is unbiased in l_2 norms,

$$\mathbb{E}_{\mathbf{M} \sim \tilde{\mathcal{D}}} [\mathbf{M}^\top (\mathbf{M}^\top \mathbf{M})^\dagger \mathbf{M}] = \frac{\tau}{d} \mathbf{I}, \quad (15)$$

then distribution \mathcal{D} of \mathbf{S} defined as $\mathbf{S}^\top \stackrel{\text{def}}{=} \mathbf{M} [\nabla^2 f(x)]^{-1/2}$ (for $\mathbf{M} \sim \tilde{\mathcal{D}}$) satisfy Assumption 1,

$$\mathbb{E}_{\mathbf{S} \sim \mathcal{D}} [\mathbf{P}_x^{\mathbf{S}}] = \frac{\tau}{d} \mathbf{I}. \quad (16)$$

2.4 Insights into theory

Before we present the main convergence results, we are going to showcase geometrically understandable auxiliary lemmas. Starting with contractive properties of a projection matrix $\mathbf{P}_x^{\mathbf{S}}$.

Lemma 4 (Contractive properties of projection matrix $\mathbf{P}_x^{\mathbf{S}}$). For any $g, h \in \mathbb{R}^d$ we have

$$\mathbb{E} \left[\|\mathbf{P}_x^{\mathbf{S}} h\|_x^2 \right] = h^\top \nabla^2 f(x) \mathbb{E} [\mathbf{P}_x^{\mathbf{S}}] h \stackrel{\text{As.1}}{=} \frac{\tau}{d} \|h\|_x^2, \quad (17)$$

$$\mathbb{E} \left[\|\mathbf{P}_x^{\mathbf{S}} g\|_x^{*2} \right] = g^\top \mathbb{E} [\mathbf{P}_x^{\mathbf{S}}] [\nabla^2 f(x)]^\dagger g \stackrel{\text{As.1}}{=} \frac{\tau}{d} \|g\|_x^{*2}, \quad (18)$$

$$\|\mathbf{P}_x^{\mathbf{S}} h\|_x^2 \leq \|\mathbf{P}_x^{\mathbf{S}} h\|_x^2 + \|(\mathbf{I} - \mathbf{P}_x^{\mathbf{S}}) h\|_x^2 = \|h\|_x^2, \quad (19)$$

$$\mathbb{E} \left[\|\mathbf{P}_x^{\mathbf{S}} h\|_x^3 \right] \leq \mathbb{E} \left[\|h\|_x \cdot \|\mathbf{P}_x^{\mathbf{S}} h\|_x^2 \right] = \|h\|_x \mathbb{E} \left[\|\mathbf{P}_x^{\mathbf{S}} h\|_x^2 \right] \stackrel{\text{As.1}}{=} \frac{\tau}{d} \|h\|_x^3. \quad (20)$$

Now we show a key idea from Regularized Newton methods: that $T_S(x, h)$ is the function value upper bound, and minimizing it in h decreases the function value.

Proposition 2 (Lemma 2 in [Hanzely et al., 2022]). For L_{semi} -semi-strong self-concordant f , and any $x \in \mathbb{R}^d$, $h \in \mathbb{R}^{\tau(\mathbf{S})}$, sketches $\mathbf{S} \in \mathbb{R}^{d \times \tau(\mathbf{S})}$ and $x_+ \stackrel{\text{def}}{=} x + \mathbf{S}h$ it holds

$$\left| f(x_+) - f(x) - \langle \nabla f(x), \mathbf{S}h \rangle - \frac{1}{2} \|\mathbf{S}h\|_x^2 \right| \leq \frac{L_{\text{semi}}}{6} \|\mathbf{S}h\|_x^3, \quad (21)$$

$$f(x_+) \leq T_{\mathbf{S}}(x, h), \quad (22)$$

hence for $h^* \stackrel{\text{def}}{=} \operatorname{argmin}_{h \in \mathbb{R}^{\tau(\mathbf{S})}} T_{\mathbf{S}}(x, h)$ and corresponding x_+ we have functional value decrease,

$$f(x_+) \leq T_{\mathbf{S}}(x, h^*) = \min_{h \in \tau(\mathbf{S})} T_{\mathbf{S}}(x, h) \leq T_{\mathbf{S}}(x, 0) = f(x).$$

Finally, we show one step decrease in local sketched norms.

Lemma 5. For $L_{\mathbf{S}}$ -self-concordant function f , updates **SGN**, (6) decrease functional value as

$$f(x_k) - f(x_{k+1}) \geq \left(2 \max \left\{ \sqrt{L_{\text{est}} \|\nabla_{\mathbf{S}_k} f(x_k)\|_{x_k, \mathbf{S}_k}^*}, 2 \right\} \right)^{-1} \|\nabla_{\mathbf{S}_k} f(x_k)\|_{x_k, \mathbf{S}_k}^{*2}. \quad (23)$$

3 Main results

Now we are ready to present the main convergence results. Firstly, Section 3.1 presents the global $\mathcal{O}(k^{-2})$ convergence rate for semi-strong self-concordant functions. Secondly, Section 3.2 demonstrates a local linear rate that is independent of problem conditioning. Thirdly, Section 3.3 shows the global linear convergence rate to a neighborhood of the solution under relative convexity assumption. Finally, Section 3.4 argues the optimality of those rates as sketch-and-project methods cannot achieve superlinear rate.

3.1 Global convex $\mathcal{O}(k^{-2})$ convergence

Denote initial level set $\mathcal{Q}(x_0) \stackrel{\text{def}}{=} \{x \in \mathbb{R}^d : f(x) \leq f(x_0)\}$. Previous lemmas imply that iterates

of **SGN** stay in $\mathcal{Q}(x_0)$, $x_k \in \mathcal{Q}(x_0) \forall k \in \mathbb{N}$. Denote its diameter $R \stackrel{\text{def}}{=} \sup_{x, y \in \mathcal{Q}(x_0)} \|x - y\|_x$.

We will present a key decrease lemma for convex setup, and the global convergence rate theorem.

Lemma 6. Fix any $y \in \mathbb{R}^d$. Let the function f be L_{semi} -semi-strong self-concordant and sketch matrices $\mathbf{S}_k \sim \mathcal{D}$ have unbiased projection matrix, Assumption 1. Then **SGN** has decrease

$$\mathbb{E}[f(x_{k+1}|x_k)] \leq \left(1 - \frac{\tau}{d}\right) f(x_k) + \frac{\tau}{d} f(y) + \frac{\tau}{d} \frac{\max L_{\text{est}} + L_{\text{semi}}}{6} \|y - x_k\|_{x_k}^3. \quad (24)$$

Theorem 2. For L_{semi} -semi-strongly concordant function f with finite diameter of initial level set $\mathcal{Q}(x_0)$, $R < \infty$ and sketching matrices with Assumption 1, **SGN** has following global convergence rate

$$\mathbb{E}[f(x_k) - f_*] \leq \frac{4d^3(f(x_0) - f_*)}{\tau^3 k^3} + \frac{9(\max L_{\text{est}} + L_{\text{semi}})d^2 R^3}{2\tau^2 k^2} = \mathcal{O}(k^{-2}). \quad (25)$$

3.2 Fast linear convergence

Without further due, we can state the fast local linear convergence theorem.

Theorem 3. Let function f be $L_{\mathbf{S}}$ -self-concordant in subspaces $\mathbf{S} \sim \mathcal{D}$ and expected projection matrix be unbiased (Assumption 1). For iterates of **SGN** x_0, \dots, x_k such that $\|\nabla_{\mathbf{S}_k} f(x_k)\|_{x_k, \mathbf{S}_k}^* \leq \frac{4}{L_{\mathbf{S}_k}}$, we have local linear convergence rate

$$\mathbb{E}[f(x_k) - f_*] \leq \left(1 - \frac{\tau}{4d}\right)^k (f(x_0) - f_*) \quad (26)$$

and the local complexity of **SGN** is independent on the problem conditioning, $\mathcal{O}\left(\frac{d}{\tau} \log \frac{1}{\varepsilon}\right)$.

3.3 Global linear convergence

Our last convergence result is a global linear rate under relative smoothness in subspaces \mathbf{S} and relative convexity. We are going to state the assumption, describe intuition, and present rates.

Definition 3. We call relative convexity and relative smoothness in subspace \mathbf{S} positive constants $\hat{\mu}, \hat{L}_{\mathbf{S}}$ for which following inequalities hold $\forall x, y \in \mathcal{Q}(x_0)$ and $h \in \mathbb{R}^{\tau(\mathbf{S})}$:

$$f(x + \mathbf{S}h) \leq f(x) + \langle \nabla_{\mathbf{S}} f(x), h \rangle + \frac{\hat{L}_{\mathbf{S}}}{2} \|h\|_{x, \mathbf{S}}^2, \quad (27)$$

$$f(y) \geq f(x) + \langle \nabla f(x), y - x \rangle + \frac{\hat{\mu}}{2} \|y - x\|_x^2. \quad (28)$$

Gower et al. [2019] shows that updates $x_+ = x + \mathbf{S}h$, where h is a minimizer of RHS of (27) converge linearly and can be written as Newton method with stepsize $\frac{1}{L}$. Conversely, our stepsize α_{k, \mathbf{S}_k} varies (9), so it is not directly applicable to us. However, a small tweak will do the trick. Observe following:

- We already have fast local convergence (Theorem 3), so we just need to show linear convergence for points $\|\nabla_{\mathbf{S}_k} f(x_k)\|_{x_k, \mathbf{S}_k}^* \geq \frac{4}{L_{\mathbf{S}_k}}$.
- For bounded stepsize α_{k, \mathbf{S}_k} smaller than $\frac{1}{L}$, we can follow global linear proof of RSN.
- Stepsize α_{k, \mathbf{S}_k} of **SGN**, (9), is inversely proportional to $L_{\text{est}} \|\nabla_{\mathbf{S}_k} f(x)\|_x^*$. Increasing L_{est} decreases the convergence neighborhood arbitrarily. We just need to express this in terms of L_{est} .
- From regularized Newton method perspective (5), we have

$$x_+ = x + \mathbf{S} \operatorname{argmin}_{h \in \mathbb{R}^{\tau(\mathbf{S})}} \left(f(x) + \langle \nabla_{\mathbf{S}} f(x), h \rangle + \frac{1}{2} \left(1 + \frac{L_{\text{est}}}{3} \|h\|_{x, \mathbf{S}} \right) \|h\|_{x, \mathbf{S}}^2 \right),$$

hence if $1 + \frac{L_{\text{est}}}{3} \|h\|_{x, \mathbf{S}} \geq \hat{L}_{\mathbf{S}}$, then (8) upperbounds on RHS of (27), and hence next iterate of **SGN** really minimizes function upperbound. Denote $\alpha_{x, \mathbf{S}}$ **SGN** stepsize in point x in range of \mathbf{S} . We express L_{est} as

$$1 + \frac{L_{\text{est}}}{3} \|h\|_{x, \mathbf{S}} \geq \hat{L}_{\mathbf{S}} \Leftrightarrow L_{\text{est}} \geq \frac{3(\hat{L}_{\mathbf{S}} - 1)}{\alpha_{k, \mathbf{S}_k} \|\nabla_{\mathbf{S}} f(x)\|_{x, \mathbf{S}}^*} \Leftrightarrow 1 \geq \frac{3(\hat{L}_{\mathbf{S}} - 1)}{-1 + \sqrt{1 + 2L_{\text{est}} \|\nabla_{\mathbf{S}} f(x)\|_{x, \mathbf{S}}^*}} \quad (29)$$

$$\Leftrightarrow L_{\text{est}} \geq \frac{3(\hat{L}_{\mathbf{S}} - 1)(3\hat{L}_{\mathbf{S}} - 1)}{2 \|\nabla_{\mathbf{S}} f(x)\|_{x, \mathbf{S}}^*}. \quad (30)$$

And for $L_{\text{est}} \geq \sup_{\mathbf{S}} \frac{9}{8} L_{\mathbf{S}} \hat{L}_{\mathbf{S}}^2 > \sup_{\mathbf{S}} \frac{3}{8} L_{\mathbf{S}} (\hat{L}_{\mathbf{S}} - 1)(3\hat{L}_{\mathbf{S}} - 1)$ it holds while $\|\nabla_{\mathbf{S}} f(x)\|_{x, \mathbf{S}}^* \geq \frac{4}{L_{\mathbf{S}}}$.

The global linear convergence rate depends on the conditioning of the expected projection matrix $\mathbf{P}_x^{\mathbf{S}}$,

$$\hat{\mathbf{P}}_x^{\mathbf{S}} \stackrel{\text{def}}{=} [\nabla^2 f(x)]^{\frac{1}{2}} \mathbf{S} [\nabla_{\mathbf{S}}^2 f(x)]^{\dagger} \mathbf{S}^{\top} [\nabla^2 f(x)]^{\frac{1}{2}} = [\nabla^2 f(x)]^{\frac{1}{2}} \mathbf{P}_x^{\mathbf{S}} [\nabla^2 f(x)]^{\dagger \frac{1}{2}}, \quad (31)$$

$$\rho(x) \stackrel{\text{def}}{=} \min_{v \in \text{Range}(\nabla^2 f(x))} \frac{v^{\top} \mathbb{E} [\alpha_{x, \mathbf{S}} \hat{\mathbf{P}}_x^{\mathbf{S}}] v}{\|v\|_{\mathbf{I}}^2} = [\nabla^2 f(x)]^{\frac{1}{2}} \mathbb{E} [\alpha_{x, \mathbf{S}} \mathbf{P}_x^{\mathbf{S}}] [\nabla^2 f(x)]^{\dagger \frac{1}{2}}, \quad (32)$$

$$\rho \stackrel{\text{def}}{=} \min_{x \in \mathcal{Q}(x_0)} \rho(x). \quad (33)$$

We can bound it and get a global convergence rate.

Theorem 4. Let f be $L_{\mathbf{S}}$ -relative smooth in subspaces \mathbf{S} and $\hat{\mu}$ -relative convex. Let sampling $\mathbf{S} \sim \mathcal{D}$ satisfy $\text{Null}(\mathbf{S}^{\top} \nabla^2 f(x) \mathbf{S}) = \text{Null}(\mathbf{S})$ and $\text{Range}(\nabla^2 f(x)) \subset \text{Range}(\mathbb{E} [\mathbf{S}_k \mathbf{S}_k^{\top}])$. Then $0 < \rho \leq 1$. Choose parameter in stepsize $L_{est} = \sup_{\mathbf{S} \sim \mathcal{D}} \frac{9}{8} L_{\mathbf{S}} \hat{L}_{\mathbf{S}}^2$. While iterates x_0, \dots, x_k satisfy $\|\nabla_{\mathbf{S}_k} f(x_k)\|_{x_k, \mathbf{S}_k}^* \geq \frac{4}{L_{\mathbf{S}_k}}$, then **SGN** has linear decrease,

$$\mathbb{E} [f(x_k) - f_*] \leq \left(1 - \frac{4}{3} \rho \hat{\mu}\right)^k (f(x_0) - f_*), \quad (34)$$

and **SGN** has global linear $\mathcal{O}\left(\frac{1}{\rho \hat{\mu}} \log \frac{1}{\varepsilon}\right)$ convergence.

3.4 Local/linear convergence limit

Similarly to AICN, we can show a quadratic decrease of the gradient norm in the sketched direction.

Lemma 7. For L_{semi} -semi-strong self-concordant function f and parameter choice $L_{est} \geq L_{semi}$, one step of **SGN** has quadratic decrease in the $\text{Range}(\mathbf{S})$,

$$\|\nabla_{\mathbf{S}} f(x_{k+1})\|_{x_k, \mathbf{S}}^* \leq L_{est} \alpha_{k, \mathbf{S}_k}^2 \|\nabla_{\mathbf{S}} f(x_k)\|_{x_k, \mathbf{S}}^{*2}. \quad (35)$$

Nevertheless, this is insufficient for superlinear local convergence; we can achieve a linear rate at best. We illustrate this on an edge case where f is a quadratic function. Then self-concordance holds with $L_{\mathbf{S}} = 0$ and as $\alpha_{k, \mathbf{S}_k} \xrightarrow{L_{\mathbf{S}} \rightarrow 0} 1$, **SGN** stepsize becomes 1 and **SGN** simplifies to subspace Newton method. Unfortunately, it has just linear local convergence [Gower et al., 2019].

4 Experiments

We support our theory by comparing **SGN** to SSCN on logistic regression empirical risk minimization:

$$\min_{x \in \mathbb{R}^d} \left\{ f(x) \stackrel{\text{def}}{=} \frac{1}{m} \sum_{i=1}^m \log \left(1 - e^{-b_i a_i^{\top} x} \right) + \frac{\mu}{2} \|x\|_2^2 \right\},$$

for data from LIBSVM [Chang and Lin, 2011], with features $\{(a_i, b_i)\}_{i=1}^m$ and labels $b_i \in \{-1, 1\}$.

To match practical considerations of SSCN and for the sake of simplicity, we adjust **SGN** in unfavorable way: **i)** we choose sketching matrices \mathbf{S} to be unbiased in l_2 norms (instead of local hessian norms $\|\cdot\|_x$ from Assumption 1). **ii)** To disregard implementation specifics, we report iterations on the x -axis. Note that SSCN needs to use a subsolver (extra line-search) to solve implicit step in each iteration. If naively implemented using matrix inverses, iterations of SSCN are $\times \log \frac{1}{\varepsilon}$ slower. We chose to didn't report time as this would naturally ask for optimized implementations and experiments on a larger scale – this was out of the scope of the paper. Figure 1 shows that despite simplicity of **SGN** and unfavourable adjustments, **SGN** performs comparably to SSCN.

We would also like to point out other properties of **SGN** based on experiments in related literature:

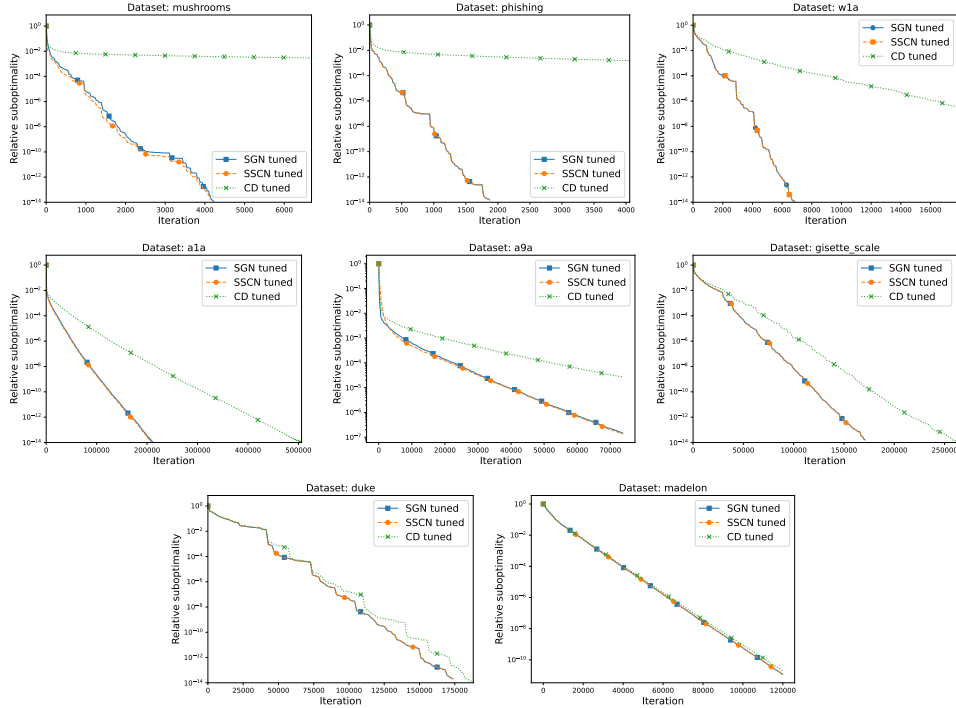


Figure 1: Comparison of SSCN, **SGN** and Coordinate Descent on logistic regression on LIBSVM datasets for sketch matrices \mathbf{S} of rank one. We fine-tune all algorithms for smoothness parameters.

- Rank of \mathbf{S} and first-order methods:** Gower et al. [2019] showed a detailed comparison of the effect of various ranks of \mathbf{S} . Also, Gower et al. [2019] showed that RSN (fixed-stepsize Newton) is much faster than first-order Accelerated Gradient Descent for highly dense problems. For extremely sparse problems, Accelerated Gradient Descent has competitive performance. As the stepsize of **SGN** is increasing while getting close to the solution, we expect similar, if not better results.

- Various sketch distributions:** Hanzely et al. [2020] considered various distributions of sketch matrices $\mathbf{S} \sim \mathcal{D}$. In all of their examples, SSCN outperformed CD with uniform or importance sampling and was competitive with Accelerated Gradient Descent. As **SGN** is competitive to SSCN, similar results should hold for **SGN** as well.

- Local norms vs l_2 norms:** Hanzely et al. [2022] shows that the optimized implementation of AICN saves time in each iteration over the optimized implementation of Cubic Newton. As **SGN** and SSCN use the same updates (but in subspaces), it indicates that **SGN** saves time over SSCN.

Acknowledgement

This project was funded by the KAUST baseline research fund of Peter Richtárik. I would like to express my sincere gratitude to Filip Hanzely and Peter Richtárik for their valuable insights and discussions regarding the limits of the setup and the related literature.

References

Jérôme Bolte and Edouard Pauwels. Curiosities and Counterexamples in Smooth Convex Optimization. *Mathematical Programming*, 195(1-2):553–603, 2022.

Chih-Chung Chang and Chih-Jen Lin. LIBSVM: A Library for Support Vector Machines. *ACM Transactions on Intelligent Systems and Technology (TIST)*, 2(3):1–27, 2011.

Andrew R Conn, Nicholas IM Gould, and Philippe L Toint. *Trust Region Methods*. SIAM, 2000.

- Nikita Doikov and Yurii Nesterov. Gradient Regularization of Newton Method with Bregman Distances. *arXiv preprint arXiv:2112.02952*, 86, 2021.
- Nikita Doikov and Yurii Nesterov. Local Convergence of Tensor Methods. *Mathematical Programming*, 193:315–336, 2022.
- Nikita Doikov and Peter Richtárik. Randomized Block Cubic Newton Method. In Jennifer Dy and Andreas Krause, editors, *The 35th International Conference on Machine Learning (ICML)*, volume 80 of *Proceedings of Machine Learning Research*, pages 1290–1298, Stockholmsmässan, Stockholm Sweden, 10–15 Jul 2018. PMLR. URL <http://proceedings.mlr.press/v80/doikov18a.html>.
- Robert M Gower and Peter Richtárik. Randomized Iterative Methods for Linear Systems. *SIAM Journal on Matrix Analysis and Applications*, 36(4):1660–1690, 2015.
- Robert M Gower, Mark Schmidt, Francis Bach, and Peter Richtárik. Variance-Reduced Methods for Machine Learning. *Proceedings of the IEEE*, 108(11):1968–1983, 2020.
- Robert Ma Gower, Dmitry Kovalev, Felix Lieder, and Peter Richtárik. RSN: Randomized Subspace Newton. In H. Wallach, H. Larochelle, A. Beygelzimer, F. d’Alché Buc, E. Fox, and R. Garnett, editors, *Advances in Neural Information Processing Systems 32*, pages 616–625. Curran Associates, Inc., 2019. URL <http://papers.nips.cc/paper/8351-rsn-randomized-subspace-newton.pdf>.
- Andreas Griewank. The Modification of Newton’s Method for Unconstrained Optimization by Bounding Cubic Terms. Technical report, Technical report NA/12, 1981.
- Filip Hanzely, Nikita Doikov, Yurii Nesterov, and Peter Richtárik. Stochastic Subspace Cubic Newton Method. In *International Conference on Machine Learning*, pages 4027–4038. PMLR, 2020.
- Slavomír Hanzely, Dmitry Kamzolov, Dmitry Pasechnyuk, Alexander Gasnikov, Peter Richtárik, and Martin Takáč. A Damped Newton Method Achieves Global $O(k^{-2})$ and Local Quadratic Convergence Rate. *Advances in Neural Information Processing Systems*, 35:25320–25334, 2022.
- Florian Jarre and Philippe L Toint. Simple Examples for the Failure of Newton’s Method with Line Search for Strictly Convex Minimization. *Mathematical Programming*, 158(1):23–34, 2016.
- Leonid Vital’evich Kantorovich. Functional Analysis and Applied Mathematics. *Uspekhi Matematicheskikh Nauk*, 3(6):89–185, 1948.
- Sai Praneeth Karimireddy, Sebastian U. Stich, and Martin Jaggi. Global Linear Convergence of Newton’s Method Without Strong-Convexity or Lipschitz Gradients. *arXiv:1806:0041*, 2018.
- Haipeng Luo, Alekh Agarwal, Nicolo Cesa-Bianchi, and John Langford. Efficient Second Order Online Learning by Sketching. *Advances in Neural Information Processing Systems*, 29, 2016.
- Walter F Mascarenhas. On the Divergence of Line Search Methods. *Computational & Applied Mathematics*, 26(1):129–169, 2007.
- Konstantin Mishchenko. Regularized Newton Method with Global $O(1/k^2)$ Convergence. *arXiv preprint arXiv:2112.02089*, 2021.
- Jorge J Moré. The Levenberg-Marquardt Algorithm: Implementation and Theory. In *Numerical Analysis*, pages 105–116. Springer, 1978.
- Yurii Nesterov and Arkadi Nemirovski. *Interior-Point Polynomial Algorithms in Convex Programming*. SIAM, 1994.
- Yurii Nesterov and Boris T Polyak. Cubic Regularization of Newton Method and Its Global Performance. *Mathematical Programming*, 108(1):177–205, 2006.

- Isaac Newton. *Philosophiae Naturalis Principia Mathematica*. Jussu Societatis Regiae ac Typis Josephi Streater, 1687.
- Roman A Polyak. Regularized Newton Method for Unconstrained Convex Optimization. *Mathematical Programming*, 120(1):125–145, 2009.
- Zheng Qu, Peter Richtárik, Martin Takáč, and Olivier Fercoq. SDNA: Stochastic dual Newton ascent for empirical risk minimization. In *The 33rd International Conference on Machine Learning (ICML)*, pages 1823–1832, 2016.
- Joseph Raphson. *Analysis Aequationum Universalis Seu Ad Aequationes Algebraicas Resolvendas Methodus Generalis & Expedita, Ex Nova Infinitarum Serierum Methodo, Deducta Ac Demonstrata*. Th. Braddyll, 1697.
- Thomas Simpson. *Essays on Several Curious and Useful Subjects, in Speculative and Mix'd Mathematicks. Illustrated by a Variety of Examples*. Printed by H. Woodfall, jun. for J. Nourse, at the Lamb without Temple-Bar, 1740.
- Tjalling J Ypma. Historical Development of the Newton–Raphson Method. *SIAM Review*, 37(4): 531–551, 1995.

Appendix

A Table of notation

A^\dagger	Moreau pseudoinverse of A
d	dimension of problem
$f : \mathbb{R}^d \rightarrow \mathbb{R}$	optimization function
$x, x_+, x_k \in \mathbb{R}^d$	iterates
$y \in \mathbb{R}^d$	virtual iterate (for analysis only)
$h, h' \in \mathbb{R}^d$	difference between consecutive iterates
x_*	optimal model
f_*	optimal function value
$\mathcal{Q}(x_0)$	set of models with functional value less than x_0
R	diameter of $\mathcal{Q}(x_0)$
$\ \cdot\ _{op}$	operator norm
$\nabla_{\mathbf{S}} f, \nabla_{\mathbf{S}}^2 f, \ h\ _{x, \mathbf{S}}$	gradient, Hessian, local norm in range \mathbf{S} , resp.
$\ \cdot\ _x$	local norm at x
$\ \cdot\ _x^*$	local dual norm at x
α_{k, \mathbf{S}_k}	SGN stepsize
$T_{\mathbf{S}}(\cdot, x)$	upperbound on f based on gradient and Hessian in x
$\mathbf{S} \in \mathbb{R}^{d \times \tau(\mathbf{S})}$	randomized sketching matrix
$\tau(\mathbf{S})$	dimension of randomized sketching matrix
τ	fixed dimension constraint on \mathbf{S}
$L_{\mathbf{S}}$	self-concordance constant in range of \mathbf{S}
$\mathbf{P}_x^{\mathbf{S}}$	projection matrix on subspace \mathbf{S} w.r.t. local norm at x
$\rho(x)$	condition numbers of expected projection matrix $\mathbb{E}[\mathbf{P}_x^{\mathbf{S}}]$
ρ	lower bound on condition numbers $\rho(x)$
L_{sc}, L_{semi}	self-concordance and semi-strong self-concordance constants, resp.
L_{est}	smoothness estimate, affects stepsize of SGN
$\hat{L}, \hat{\mu}$	relative smoothness and relative convexity constants

Table 4: Table of notation

B Experiments: technical details and extra comparison

For completeness, in Figure 2 we include comparison of **SGN** and Accelerated Coordinate Descent on small-scale experiments.

We use comparison framework from [Hanzely et al., 2020], including implementations of SSCN, Coordinate Descent and Accelerated Coordinate Descent.

Experiments are implemented in Python 3.6.9 and run on workstation with 48 CPUs Intel(R) Xeon(R) Gold 6246 CPU @ 3.30GHz. Total training time was less than 10 hours. Source code and instructions are included in supplementary materials. As we fixed random seed, experiments should be fully reproducible.

C Algorithm comparisons

For readers convenience, we include pseudocodes of the most relevant baseline algorithms: Exact Newton Descent (Algorithm 2), RSN (Algorithm 3), SSCN (Algorithm 4), AICN (Algorithm 5).

We include extended version of Table 1 in Table 5.

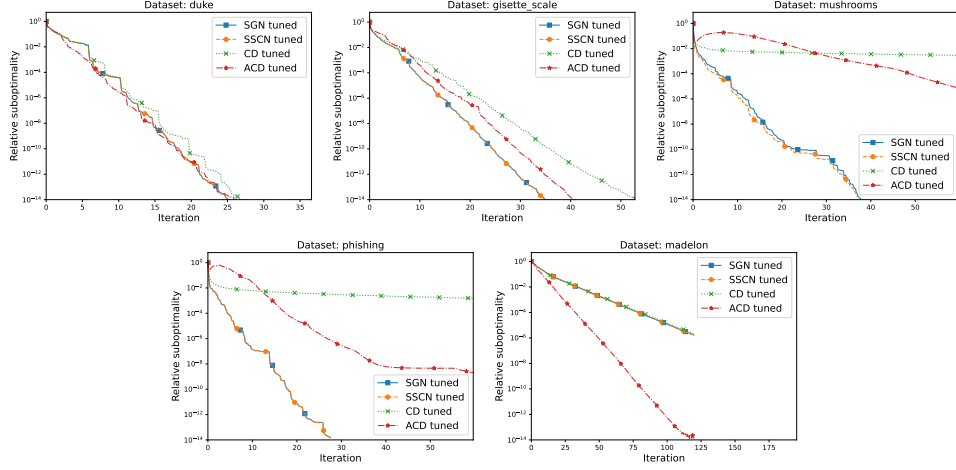


Figure 2: Comparison of SSCN, **SGN**, Coordinate Descent and Accelerated Coordinate Descent on logistic regression on LIBSVM datasets for sketch matrices \mathbf{S} of rank one. We fine-tune all algorithms for smoothness parameters.

Algorithm 2 Exact Newton Descent [Karimireddy et al., 2018]

Requires: Initial point $x_0 \in \mathbb{R}^d$, c -stability bound $\sigma > c > 0$
for $k = 0, 1, 2 \dots$ **do**
 $x_{k+1} = x_k - \frac{1}{\sigma} [\nabla^2 f(x_k)]^\dagger \nabla f(x_k)$
end for

Algorithm 3 Randomized Subspace Newton [Gower et al., 2019]

Requires: Initial point $x_0 \in \mathbb{R}^d$, distribution of sketches \mathcal{D} , relative smoothness constant $L_{\text{rel}} > 0$
for $k = 0, 1, 2 \dots$ **do**
Sample $\mathbf{S}_k \sim \mathcal{D}$
 $x_{k+1} = x_k - \frac{1}{L_{\text{rel}}} \mathbf{S}_k [\nabla_{\mathbf{S}_k}^2 f(x_k)]^\dagger \nabla_{\mathbf{S}_k} f(x_k)$
end for

Algorithm 4 SSCN: Stochastic Subspace Cubic Newton [Hanzely et al., 2020]

Requires: Initial point $x_0 \in \mathbb{R}^d$, distribution of random matrices \mathcal{D} , Lipschitzness of Hessian constant $L_{\mathbf{S}} > 0$
for $k = 0, 1, 2 \dots$ **do**
Sample $\mathbf{S}_k \sim \mathcal{D}$
 $x_{k+1} = x_k - \mathbf{S}_k \operatorname{argmin}_{h \in \mathbb{R}^d} \hat{T}_{\mathbf{S}_k}(x_k, h)^a$
end for

^afor $\hat{T}_{\mathbf{S}}(x, h) = \langle \nabla f(x), \mathbf{S}h \rangle + \frac{1}{2} \|\mathbf{S}h\|_x^2 + \frac{L_{\mathbf{S}}}{6} \|\mathbf{S}h\|_x^3$

Algorithm 5 Affine-Invariant Cubic Newton [Hanzely et al., 2022]

Requires: Initial point $x_0 \in \mathbb{R}^d$, estimate of semi-strong self-concordance $L_{\text{est}} \geq L_{\text{semi}} > 0$
for $k = 0, 1, 2 \dots$ **do**
 $\alpha_k = \frac{-1 + \sqrt{1 + 2L_{\text{est}} \|\nabla f(x_k)\|_{x_k}^*}}{L_{\text{est}} \|\nabla f(x_k)\|_{x_k}^*}$
 $x_{k+1} = x_k - \alpha_k [\nabla^2 f(x_k)]^{-1} \nabla f(x_k)^a$
end for

^aEquivalent, $x_{k+1} = x_k - \operatorname{argmin}_{h \in \mathbb{R}^d} T(x_k, h)$, for $T(x, h) \stackrel{\text{def}}{=} \langle \nabla f(x), h \rangle + \frac{1}{2} \|h\|_x^2 + \frac{L_{\text{est}}}{6} \|h\|_x^3$

Table 5: Global convergence rate of low-rank Newton methods for convex and Lipschitz smooth functions. We use fastest full-dimensional algorithms as the baseline (for extended version, see Section 4). For simplicity, we disregard differences between various notions of smoothness.

Update direction	Update oracle (direction is deterministic)	Low-rank (direction in expectation)
Non-Newton direction	$\mathcal{O}(\mathbf{k}^{-2})$ Cubic Newton [Nesterov and Polyak, 2006] Glob. Regularized Newton [Mishchenko, 2021] [Doikov and Nesterov, 2021]	$\mathcal{O}(k^{-1})$ Stoch. Subspace Cubic Newton [Hanzely et al., 2020]
Newton direction	$\mathcal{O}(k^{-\frac{1}{4}})$ Globally Regularized Newton [Polyak, 2009]	$\mathcal{O}(\mathbf{k}^{-2})$ Sketchy Global Newton (this work) $\mathcal{O}(k^{-1})$ Randomized Subspace Newton [Gower et al., 2019]
	$\mathcal{O}(\mathbf{k}^{-2})$ Affine-Invariant Cubic Newton [Hanzely et al., 2022] $\mathcal{O}(k^{-1})$ Exact Newton Descent [Karimireddy et al., 2018] $\mathcal{O}(k^{-\frac{1}{2}})$ Damped Newton B [Nesterov and Nemirovski, 1994]	

D Proofs

For easier reference, we split proofs into four sections, based on the result category:

- Proofs explaining general properties of **SGN** (Appendix D.1)
- Proofs of global rate $\mathcal{O}(k^{-2})$ in convex setup (Appendix D.2)
- Proofs of local linear rate (Appendix D.3)
- Proofs of global linear rate (Appendix D.4)

D.1 General properties

Proof of Theorem 1. (Three viewpoints of **SGN**)

Because $\nabla f(x_k) \in \text{Range}(\nabla^2 f(x_k))$, it holds $\nabla^2 f(x_k)[\nabla^2 f(x_k)]^\dagger \nabla f(x_k) = \nabla f(x_k)$. Updates (6) and (7) are equivalent as

$$\begin{aligned} \mathbf{P}_{x_k}^{\mathbf{S}_k} [\nabla^2 f(x_k)]^\dagger \nabla f(x_k) &= \mathbf{S}_k (\mathbf{S}_k^\top \nabla^2 f(x_k) \mathbf{S}_k)^\dagger \mathbf{S}_k^\top \nabla^2 f(x_k) [\nabla^2 f(x_k)]^\dagger \nabla f(x_k) \\ &= \mathbf{S}_k (\mathbf{S}_k^\top \nabla^2 f(x_k) \mathbf{S}_k)^\dagger \mathbf{S}_k^\top \nabla f(x_k) \\ &= \mathbf{S}_k [\nabla_{\mathbf{S}_k}^2 f(x_k)]^\dagger \nabla_{\mathbf{S}_k} f(x_k) \end{aligned}$$

Taking gradient of $T_{\mathbf{S}_k}(x_k, h)$ w.r.t. h and setting it to 0 yields that for solution h^* holds

$$\nabla_{\mathbf{S}_k} f(x_k) + \nabla_{\mathbf{S}_k}^2 f(x_k) h^* + \frac{L_{\text{est}}}{2} \|h^*\|_{x_k, \mathbf{S}_k} \nabla_{\mathbf{S}_k}^2 f(x_k) h^* = 0 \quad (36)$$

which after rearranging is

$$h^* = - \left(1 + \frac{L_{\text{est}}}{2} \|h^*\|_{x_k, \mathbf{S}_k} \right)^{-1} [\nabla_{\mathbf{S}_k}^2 f(x_k)]^\dagger \nabla_{\mathbf{S}_k} f(x_k), \quad (37)$$

thus solution of cubical regularization in local norms (8) has form of Newton method with stepsize $\alpha_{k, \mathbf{S}_k} = \left(1 + \frac{L_{\text{est}}}{2} \|h^*\|_{x_k, \mathbf{S}_k} \right)^{-1}$. We are left to show that this α_{k, \mathbf{S}_k} is equivalent to (9).

Substitute h^* from (37) to (36) and $\alpha_{k, \mathbf{S}_k} = \left(1 + \frac{L_{\text{est}}}{2} \|h^*\|_{x_k, \mathbf{S}_k} \right)^{-1}$ and then use $\nabla^2 f(x_k)[\nabla^2 f(x_k)]^\dagger \nabla f(x_k) = \nabla f(x_k)$, to get

$$0 = \nabla_{\mathbf{S}_k} f(x_k) + \nabla_{\mathbf{S}_k}^2 f(x_k) \left(-\alpha_{k, \mathbf{S}_k} [\nabla_{\mathbf{S}_k}^2 f(x_k)]^\dagger \nabla_{\mathbf{S}_k} f(x_k) \right) \quad (38)$$

$$+ \frac{L_{\text{est}}}{2} \left(\alpha_{k, \mathbf{S}_k} \|\nabla_{\mathbf{S}_k} f(x_k)\|_{x_k, \mathbf{S}_k}^* \right) \nabla_{\mathbf{S}_k}^2 f(x_k) \left(-\alpha_{k, \mathbf{S}_k} [\nabla_{\mathbf{S}_k}^2 f(x_k)]^\dagger \nabla_{\mathbf{S}_k} f(x_k) \right) \quad (39)$$

$$= \left(1 - \alpha_{k, \mathbf{S}_k} - \frac{L_{\text{est}}}{2} \alpha_{k, \mathbf{S}_k}^2 \|\nabla_{\mathbf{S}_k} f(x_k)\|_{x_k, \mathbf{S}_k}^* \right) \nabla_{\mathbf{S}_k} f(x_k). \quad (40)$$

Finally, α_{k, \mathbf{S}_k} from (9) is a positive root of polynomial $1 - \alpha_{k, \mathbf{S}_k} - \frac{L_{\text{est}}}{2} \alpha_{k, \mathbf{S}_k}^2 = 0$, which concludes the equivalence of (6), (7) and (5). \square

Lemma 8 (Stepsize bound). *Stepsize α_{k, \mathbf{S}_k} can be bounded as*

$$\alpha_{k, \mathbf{S}_k} \leq \frac{\sqrt{2}}{\sqrt{L_{\text{est}} \|\nabla_{\mathbf{S}_k} f(x_k)\|_{x_k, \mathbf{S}_k}^*}}, \quad (41)$$

and for x_k far from solution, $\|\nabla_{\mathbf{S}_k} f(x_k)\|_{x_k, \mathbf{S}_k}^* \geq \frac{4}{L_{\text{S}_k}}$ and $L_{\text{est}} = \frac{9}{8} \sup_{\mathbf{S}} L_{\mathbf{S}} \hat{L}_{\mathbf{S}}^2$ holds $\alpha_{k, \mathbf{S}_k} \hat{L}_{\mathbf{S}_k} \leq \frac{2}{3}$.

Proof of Lemma 1. (Matrix $\mathbf{P}_x^{\mathbf{S}}$ is a projection matrix)

For arbitrary square matrix \mathbf{M} pseudoinverse guarantee $\mathbf{M}^\dagger \mathbf{M} \mathbf{M}^\dagger = \mathbf{M}^\dagger$. Applying this to $M \leftarrow (\mathbf{S}^\top \nabla^2 f(x) \mathbf{S})$ yields $\langle \mathbf{P}_x^{\mathbf{S}} y, \mathbf{P}_x^{\mathbf{S}} z \rangle_{\nabla^2 f(x)} = \langle \mathbf{P}_x^{\mathbf{S}} y, z \rangle_{\nabla^2 f(x)}$, $y, z \in \mathbb{R}^d$. Thus, $\mathbf{P}_x^{\mathbf{S}}$ is really projection matrix w.r.t. $\|\cdot\|_x$. \square

Proof of Lemma 2. (Unbiased $\mathbf{P}_x^{\mathbf{S}}$ implies $\mathbb{E}[\tau(\mathbf{S})] = \tau$, as in Lemma 5.2 of [Hanzely et al., 2020]) We use definitions and cyclic property of the matrix trace,

$$\mathbb{E}[\tau(\mathbf{S})] = \mathbb{E}[\text{Tr}(\mathbf{I}^\top(\mathbf{S}))] = \mathbb{E}[\text{Tr}(\mathbf{S}^\top \nabla^2 f(x) \mathbf{S} (\mathbf{S}^\top \nabla^2 f(x) \mathbf{S})^\dagger)] = \mathbb{E}[\text{Tr}(\mathbf{P}_x^{\mathbf{S}})] \quad (42)$$

$$= \text{Tr}\left(\frac{\tau}{d} \mathbf{I}^d\right) = \tau. \quad (43)$$

\square

Proof of Lemma 3. (Construction of unbiased sketch matrices in local norms from ones in l_2 norms) We have

$$\mathbb{E}_{\mathbf{S} \sim \mathcal{D}}[\mathbf{P}_x^{\mathbf{S}}] = [\nabla^2 f(x)]^{-1/2} \mathbb{E}_{\mathbf{M} \sim \tilde{\mathcal{D}}}[\mathbf{M}^\top (\mathbf{M}^\top \mathbf{M})^\dagger \mathbf{M}] [\nabla^2 f(x)]^{1/2} \quad (44)$$

$$= [\nabla^2 f(x)]^{-1/2} \frac{\tau}{d} \mathbf{I} [\nabla^2 f(x)]^{1/2} = \frac{\tau}{d} \mathbf{I}. \quad (45)$$

\square

Proof of Lemma 5. (One step functional value decrease in terms of norms of gradients)

For $h_k = x_{k+1} - x_k$, we can follow proof of Lemma 10 in Hanzely et al. [2022],

$$f(x_k) - f(x_{k+1}) \stackrel{(21)}{\geq} -\langle \nabla_{\mathbf{S}} f(x_k), h_k \rangle - \frac{1}{2} \|h_k\|_{x_k, \mathbf{S}_k}^2 - \frac{L_{\text{est}}}{6} \|h_k\|_{x_k, \mathbf{S}_k}^3 \quad (46)$$

$$\stackrel{(10)}{=} \alpha_{k, \mathbf{S}_k} \|\nabla_{\mathbf{S}_k} f(x_k)\|_{x_k, \mathbf{S}_k}^{*2} - \frac{1}{2} \alpha_{k, \mathbf{S}_k}^2 \|\nabla_{\mathbf{S}_k} f(x_k)\|_{x_k, \mathbf{S}_k}^{*2} \quad (47)$$

$$- \frac{L_{\text{est}}}{6} \alpha_{k, \mathbf{S}_k}^3 \|\nabla_{\mathbf{S}_k} f(x_k)\|_{x_k, \mathbf{S}_k, \mathbf{S}}^{*3} \quad (48)$$

$$= \left(1 - \frac{1}{2} \alpha_{k, \mathbf{S}_k} - \frac{L_{\text{est}}}{6} \alpha_{k, \mathbf{S}_k}^2 \|\nabla_{\mathbf{S}_k} f(x_k)\|_{x_k, \mathbf{S}_k}^*\right) \alpha_{k, \mathbf{S}_k} \|\nabla_{\mathbf{S}_k} f(x_k)\|_{x_k, \mathbf{S}_k}^{*2} \quad (49)$$

$$\geq \frac{1}{2} \alpha_{k, \mathbf{S}_k} \|\nabla_{\mathbf{S}_k} f(x_k)\|_{x_k, \mathbf{S}_k}^{*2} \quad (50)$$

$$\geq \frac{1}{2 \max\left\{\sqrt{L_{\text{est}} \|\nabla_{\mathbf{S}_k} f(x_k)\|_{x_k, \mathbf{S}_k}^*}, 2\right\}} \|\nabla_{\mathbf{S}_k} f(x_k)\|_{x_k, \mathbf{S}_k}^{*2}. \quad (51)$$

\square

Proof of Lemma 7. (Quadratic local decrease in subspaces).

We bound norm of $\nabla_{\mathbf{S}} f(x_{k+1})$ using basic norm manipulation and triangle inequality as

$$\begin{aligned} & \|\nabla_{\mathbf{S}_k} f(x_{k+1})\|_{x_k, \mathbf{S}_k}^* \\ &= \|\nabla_{\mathbf{S}_k} f(x_{k+1}) - \nabla_{\mathbf{S}_k}^2 f(x_k)(x_{k+1} - x_k) - \alpha_{k, \mathbf{S}_k} \nabla_{\mathbf{S}_k} f(x_k)\|_{x_k, \mathbf{S}_k}^* \\ &= \|\nabla_{\mathbf{S}_k} f(x_{k+1}) - \nabla_{\mathbf{S}_k} f(x_k) - \nabla_{\mathbf{S}_k}^2 f(x_k)(x_{k+1} - x_k) + (1 - \alpha_{k, \mathbf{S}_k}) \nabla_{\mathbf{S}_k} f(x_k)\|_{x_k, \mathbf{S}_k}^* \\ &\leq \|\nabla_{\mathbf{S}_k} f(x_{k+1}) - \nabla_{\mathbf{S}_k} f(x_k) - \nabla_{\mathbf{S}_k}^2 f(x_k)(x_{k+1} - x_k)\|_{x_k, \mathbf{S}_k}^* + (1 - \alpha_{k, \mathbf{S}_k}) \|\nabla_{\mathbf{S}_k} f(x_k)\|_{x_k, \mathbf{S}_k}^* \end{aligned}$$

Using L_{semi} -semi-strong self-concordance, we can continue

$$\begin{aligned}
&\leq \|\nabla_{\mathbf{S}_k} f(x_{k+1}) - \nabla_{\mathbf{S}_k} f(x_k) - \nabla_{\hat{\mathbf{S}}_k}^2 f(x_k)(x_{k+1} - x_k)\|_{x_k, \mathbf{S}_k}^* + (1 - \alpha_{k, \mathbf{S}_k}) \|\nabla_{\mathbf{S}_k} f(x_k)\|_{x_k, \mathbf{S}_k}^* \\
&\leq \frac{L_{\text{semi}}}{2} \|x_{k+1} - x_k\|_{x_k, \mathbf{S}_k}^2 + (1 - \alpha_{k, \mathbf{S}_k}) \|\nabla_{\mathbf{S}_k} f(x_k)\|_{x_k, \mathbf{S}_k}^* \\
&= \frac{L_{\text{semi}} \alpha_{k, \mathbf{S}_k}^2}{2} \|\nabla_{\mathbf{S}_k} f(x_k)\|_{x_k, \mathbf{S}_k}^{*2} + (1 - \alpha_{k, \mathbf{S}_k}) \|\nabla_{\mathbf{S}_k} f(x_k)\|_{x_k, \mathbf{S}_k}^* \\
&\leq \frac{L_{\text{est}} \alpha_{k, \mathbf{S}_k}^2}{2} \|\nabla_{\mathbf{S}_k} f(x_k)\|_{x_k, \mathbf{S}_k}^{*2} + (1 - \alpha_{k, \mathbf{S}_k}) \|\nabla_{\mathbf{S}_k} f(x_k)\|_{x_k, \mathbf{S}_k}^* \\
&= \left(\frac{L_{\text{est}} \alpha_{k, \mathbf{S}_k}^2}{2} \|\nabla_{\mathbf{S}_k} f(x_k)\|_{x_k, \mathbf{S}_k}^* - \alpha_{k, \mathbf{S}_k} + 1 \right) \|\nabla_{\mathbf{S}_k} f(x_k)\|_{x_k, \mathbf{S}_k}^* \\
&\stackrel{(9)}{=} L_{\text{est}} \alpha_{k, \mathbf{S}_k}^2 \|\nabla_{\mathbf{S}_k} f(x_k)\|_{x_k, \mathbf{S}_k}^{*2}.
\end{aligned}$$

Last equality holds because of the choice of α_{k, \mathbf{S}_k} . \square

D.1.1 Technical lemmas

Lemma 9 (Arithmetic mean – Geometric mean inequality). *For $c \geq 0$ we have*

$$1 + c = \frac{1 + (1 + 2c)}{2} \stackrel{AG}{\geq} \sqrt{1 + 2c}. \quad (52)$$

Lemma 10 (Jensen for square root). *Function $f(x) = \sqrt{x}$ is concave, hence for $c \geq 0$ we have*

$$\frac{1}{\sqrt{2}}(\sqrt{c} + 1) \leq \sqrt{c + 1} \leq \sqrt{c} + 1. \quad (53)$$

Proof of Lemma 8. Denote $G_k \stackrel{\text{def}}{=} L_{\text{est}} \|\nabla_{\mathbf{S}_k} f(x_k)\|_{x_k, \mathbf{S}_k}^*$. Using (53) with $c \leftarrow 2G > 0$ and

$$\alpha_{k, \mathbf{S}_k} = \frac{-1 + \sqrt{1 + 2G}}{G} \leq \frac{\sqrt{2G}}{G} = \frac{\sqrt{2}}{\sqrt{G}} = \frac{\sqrt{2}}{\sqrt{L_{\text{est}} \|\nabla_{\mathbf{S}_k} f(x_k)\|_{x_k, \mathbf{S}_k}^*}} \quad (54)$$

and

$$\alpha_{k, \mathbf{S}_k} \hat{L}_{\mathbf{S}_k} \leq \frac{\sqrt{2} \hat{L}_{\mathbf{S}_k}}{\sqrt{L_{\text{est}} \|\nabla_{\mathbf{S}_k} f(x_k)\|_{x_k, \mathbf{S}_k}^*}} \quad (55)$$

$$\leq \frac{\sqrt{2} \hat{L}_{\mathbf{S}_k}}{\sqrt{\frac{9}{8} L_{\mathbf{S}_k} \hat{L}_{\mathbf{S}_k}^2 \|\nabla_{\mathbf{S}_k} f(x_k)\|_{x_k, \mathbf{S}_k}^*}} \quad (56)$$

$$\leq \frac{4}{3} \frac{1}{\sqrt{L_{\mathbf{S}_k} \|\nabla_{\mathbf{S}_k} f(x_k)\|_{x_k, \mathbf{S}_k}^*}} \leq \frac{2}{3} \quad \text{for } \|\nabla_{\mathbf{S}_k} f(x_k)\|_{x_k, \mathbf{S}_k}^* \geq \frac{4}{\hat{L}_{\mathbf{S}_k}}. \quad (57)$$

\square

D.2 Global convex rate

Proof of Lemma 6. (Key lemma for global convex convergence). Denote

$$\Omega_{\mathbf{S}}(x, h') \stackrel{\text{def}}{=} f(x) \langle \nabla f(x), \mathbf{P}_x^{\mathbf{S}} h' \rangle + \frac{1}{2} \|\mathbf{P}_x^{\mathbf{S}} h'\|_x^2 + \frac{L_{\text{est}}}{6} \|\mathbf{P}_x^{\mathbf{S}} h'\|_x^3, \quad (58)$$

so that

$$\min_{h' \in \mathbb{R}^d} \Omega_{\mathbf{S}}(x, h') = \min_{h \in \mathbb{R}^{\tau(\mathbf{S})}} T_{\mathbf{S}}(x, h). \quad (59)$$

For arbitrary $y \in \mathbb{R}^d$ denote $h \stackrel{\text{def}}{=} y - x_k$. We can calculate

$$f(x_{k+1}) \leq \min_{h' \in \mathbb{R}^{\tau(\mathbf{S})}} T_{\mathbf{S}}(x_k, h') = \min_{h'' \in \mathbb{R}^d} \Omega_{\mathbf{S}}(x_k, h'') \quad (60)$$

$$\mathbb{E}[f(x_{k+1})] \leq \mathbb{E}[\Omega_{\mathbf{S}}(x_k, h)] \quad (61)$$

$$= f(x_k) + \frac{\tau}{d} \langle \nabla f(x_k), h \rangle + \frac{1}{2} \mathbb{E} \left[\|\mathbf{P}_x^{\mathbf{S}} h\|_{x_k}^2 \right] + \mathbb{E} \left[\frac{L_{\text{est}}}{6} \|\mathbf{P}_x^{\mathbf{S}} h\|_{x_k}^3 \right] \quad (62)$$

$$\stackrel{(17)}{\leq} f(x_k) + \frac{\tau}{d} \langle \nabla f(x_k), h \rangle + \frac{\tau}{2d} \|h\|_{x_k}^2 + \frac{L_{\text{est}} \tau}{6} \|h\|_{x_k}^3 \quad (63)$$

$$\stackrel{(21)}{\leq} f(x_k) + \frac{\tau}{d} \left(f(y) - f(x_k) + \frac{L_{\text{semi}}}{6} \|y - x_k\|_{x_k}^3 \right) + \frac{L_{\text{est}} \tau}{6} \|h\|_{x_k}^3, \quad (64)$$

In second to last inequality depends on unbiasedness of projection $\mathbf{P}_x^{\mathbf{S}}$, Assumption 1. In last inequality we used semi-strong self-concordance, Proposition 2 with $\mathbf{S} = \mathbf{I}$. \square

Proof of Theorem 2. (Global convex rate). Denote

$$A_0 \stackrel{\text{def}}{=} \frac{4}{3} \left(\frac{d}{\tau} \right)^3, \quad (65)$$

$$A_k \stackrel{\text{def}}{=} A_0 + \sum_{t=1}^k t^2 = A_0 - 1 + \frac{k(k+1)(2k+1)}{6} \geq A_0 + \frac{k^3}{3}, \quad (66)$$

$$\dots \text{consequently} \quad \sum_{t=1}^k \frac{t^6}{A_t^2} \leq 9k, \quad (67)$$

$$\eta_t \stackrel{\text{def}}{=} \frac{d}{\tau} \frac{(t+1)^2}{A_{t+1}} \quad \text{implying} \quad 1 - \frac{d}{\tau} \eta_t = \frac{A_t}{A_{t+1}}. \quad (68)$$

Note that this choice of A_0 implies [Hanzely et al., 2020]

$$\eta_{t-1} \leq \frac{d}{\tau} \frac{t^2}{A_0 + \frac{t^3}{3}} \leq \frac{d}{\tau} \sup_{t \in \mathbb{N}} \frac{t^2}{A_0 + \frac{t^3}{3}} \leq \frac{d}{\tau} \sup_{\zeta > 0} \frac{\zeta^2}{A_0 + \frac{\zeta^3}{3}}, = 1 \quad (69)$$

and $\eta_t \in [0, 1]$. Set $y \stackrel{\text{def}}{=} \eta_t x_* + (1 - \eta_t) x_t$ in Lemma 6. From convexity of f ,

$$\mathbb{E}[f(x_{t+1}|x_t)] \leq \left(1 - \frac{\tau}{d}\right) f(x_t) + \frac{\tau}{d} f_* \eta_t + \frac{\tau}{d} f(x_t) (1 - \eta_t) + \frac{\tau}{d} \left(\frac{\max L_{\mathbf{S}} + L_{\text{semi}}}{6} \|x_t - x_*\|_{x_t}^3 \eta_t^3 \right). \quad (70)$$

Denote $\delta_t \stackrel{\text{def}}{=} \mathbb{E}[f(x_t) - f_*]$. Subtracting f_* from both sides and substituting η_k yields

$$\delta_{t+1} \leq \frac{A_t}{A_{t+1}} \delta_t + \frac{\max L_{\mathbf{S}} + L_{\text{semi}}}{6} \|x_t - x_*\|_{x_t}^3 \left(\frac{d}{\tau} \right)^2 \left(\frac{(t+1)^2}{A_{t+1}} \right)^3. \quad (71)$$

Multiplying by A_{t+1} and summing from from $t = 0, \dots, k-1$ yields

$$A_k \delta_k \leq A_0 \delta_0 + \frac{\max L_{\mathbf{S}} + L_{\text{semi}}}{6} \frac{d^2}{\tau^2} \sum_{t=0}^{k-1} \|x_t - x_*\|_{x_t}^3 \frac{(t+1)^6}{A_{t+1}^2}, \quad (72)$$

Using $\sup_{x \in \mathcal{Q}(x_0)} \|x - x_*\|_x \leq R$ we can simplify and shift summation indices,

$$A_k \delta_k \leq A_0 \delta_0 + \frac{\max L_{\mathbf{S}} + L_{\text{semi}}}{6} \frac{d^2}{\tau^2} D^3 \sum_{t=1}^k \frac{t^6}{A_t^2} \quad (73)$$

$$\leq A_0 \delta_0 + \frac{\max L_{\mathbf{S}} + L_{\text{semi}}}{6} \frac{d^2}{\tau^2} D^3 9k \quad (74)$$

and

$$\delta_k \leq \frac{A_0 \delta_0}{A_k} + \frac{3(\max L_{\mathbf{S}} + L_{\text{semi}})d^2 D^3 k}{2\tau^2 A_k} \quad (75)$$

$$\leq \frac{3A_0 \delta_0}{k^3} + \frac{9(\max L_{\mathbf{S}} + L_{\text{semi}})d^2 D^3}{2\tau^2 k^2} \quad (76)$$

which concludes the proof. \square

D.3 Local linear rate

Proposition 3 (Lemma E.3 in Hanzely et al. [2020]). *For $\gamma > 0$ and x_k in neighborhood $x_k \in \left\{x : \|\nabla f(x)\|_x^* < \frac{2}{(1+\gamma^{-1})L_{sc}}\right\}$ for L_{sc} -self-concordant function f , we can bound*

$$f(x_k) - f_* \leq \frac{1}{2}(1+\gamma)\|\nabla f(x_k)\|_{x_k}^{*2}. \quad (77)$$

Proof of Theorem 3. (Fast local linear rate theorem).

Proposition 3 with $\gamma = 2$ implies that in neighborhood $\|\nabla f(x_k)\|_{x_k, \mathbf{S}}^{*2} \leq \frac{4}{L_{\mathbf{S}}}$,

$$f(x_k) - f(x_{k+1}) \stackrel{(23)}{\geq} \frac{1}{4}\|\nabla_{\mathbf{S}_k} f(x_k)\|_{x_k, \mathbf{S}_k}^{*2}$$

and with identity $\|\nabla_{\mathbf{S}} f(x)\|_{x, \mathbf{S}_k}^{*2} = \|\mathbf{P}_x^{\mathbf{S}} \nabla f(x)\|_x^{*2}$, we can continue

$$\mathbb{E}[f(x_k) - f(x_{k+1})] \stackrel{(23)}{\geq} \mathbb{E}\left[\frac{1}{4}\|\nabla_{\mathbf{S}_k} f(x_k)\|_{x_k, \mathbf{S}}^{*2}\right] = \mathbb{E}\left[\frac{1}{4}\|\mathbf{P}_{x_k}^{\mathbf{S}_k} \nabla f(x_k)\|_{x_k}^{*2}\right] \quad (78)$$

$$\stackrel{(18)}{=} \frac{\tau}{4d}\|\nabla f(x_k)\|_{x_k}^{*2} \stackrel{(77)}{\geq} \frac{\tau}{2d(1+\gamma)}(f(x_k) - f_*). \quad (79)$$

Hence

$$\mathbb{E}[f(x_{k+1}) - f_*] \leq \left(1 - \frac{\tau}{2d(1+\gamma)}\right)(f(x_k) - f_*),$$

and to finish the proof, we use tower property across iterates x_0, x_1, \dots, x_k . \square

D.4 Global linear rate

Proposition 4 ((47) in Gower et al. [2019]). *Relative convexity (28) implies following bound*

$$f_* \leq f(x_k) - \frac{1}{2\hat{\rho}}\|\nabla f(x_k)\|_{x_k}^{*2}. \quad (80)$$

Proposition 5 (Analogy to Lemma 7 in [Gower et al., 2019]). *For $\mathbf{S} \sim \mathcal{D}$ satisfying conditions*

$$\text{Null}(\mathbf{S}^\top \nabla^2 f(x) \mathbf{S}) = \text{Null}(\mathbf{S}) \quad \text{and} \quad \text{Range}(\nabla^2 f(x)) \subset \text{Range}(\mathbb{E}[\mathbf{S}_k \mathbf{S}_k^\top]), \quad (81)$$

also exactness condition holds

$$\text{Range}(\nabla^2 f(x)) = \text{Range}\left(\mathbb{E}\left[\hat{\mathbf{P}}_x^{\mathbf{S}}\right]\right), \quad (82)$$

and formula for $\rho(x)$ can be simplified

$$\rho(x) = \lambda_{\min}^+(\mathbb{E}[\alpha_{x, \mathbf{S}} \mathbf{P}_x^{\mathbf{S}}]) > 0 \quad (83)$$

and bounded $0 < \rho(x) \leq 1$. Consequently, $0 < \rho \leq 1$.

Proof of Theorem 4. (Global linear convergence under relative convexity)

Replacing $x \leftarrow x_k$ and $h \leftarrow \alpha_{k, \mathbf{S}_k} \mathbf{P}_{x_k}^{\mathbf{S}_k} [\nabla^2 f(x_k)]^\dagger \nabla f(x_k)$ so that $x_{k+1} = x_k + \mathbf{S}h$ in (27) yields

$$f(x_{k+1}) \leq f(x_k) - \alpha_{k, \mathbf{S}_k} \left(1 - \frac{1}{2} \hat{L}_{\mathbf{S}_k} \alpha_{k, \mathbf{S}_k} \right) \|\nabla_{\mathbf{S}_k} f(x_k)\|_{x_k, \mathbf{S}_k}^{*2} \quad (84)$$

$$\leq f(x_k) - \frac{2}{3} \alpha_{k, \mathbf{S}_k} \|\nabla_{\mathbf{S}_k} f(x_k)\|_{x_k, \mathbf{S}_k}^{*2}. \quad (85)$$

In last step, we used that $\hat{L}_{\mathbf{S}_k} \alpha_{k, \mathbf{S}_k} \leq \frac{2}{3}$ holds for $\|\nabla_{\mathbf{S}_k} f(x_k)\|_{x_k, \mathbf{S}_k}^* \geq \frac{4}{\hat{L}_{\mathbf{S}_k}}$ (Lemma 8). Next, we take expectation on x_k and use definition of $\rho(x_k)$.

$$\mathbb{E}[f(x_{k+1})] \leq f(x_k) - \frac{2}{3} \|\nabla f(x_k)\|_{x_k}^2 \mathbb{E} \left[\alpha_{k, \mathbf{S}_k} \mathbf{S} [\nabla_{\mathbf{S}_k}^2 f(x_k)]^\dagger \mathbf{S}^\top \right] \quad (86)$$

$$\leq f(x_k) - \frac{2}{3} \rho(x_k) \|\nabla f(x_k)\|_{x_k}^{*2} \quad (87)$$

$$\stackrel{(80)}{\leq} f(x_k) - \frac{4}{3} \rho(x_k) \hat{\mu} (f(x_k) - f_*). \quad (88)$$

Now $\rho(x) \geq \rho$, and ρ is bounded in Proposition 5. Rearranging and subtracting f_* gives

$$\mathbb{E}[f(x_{k+1}) - f_*] \leq \left(1 - \frac{4}{3} \rho \hat{\mu} \right) (f(x_k) - f_*), \quad (89)$$

Which after towering across all iterates yields the statement. \square